High-order harmonic generation by one- and two-electron molecular ions with intense laser pulses

André D. Bandrauk and Hengtai Yu
Laboratoire de Chimie Théorique, Faculté des Sciences, Université de Sherbrooke, Sherbrooke, Québec, Canada J1K 2R1
(Received 16 March 1998)

Numerical solutions of the time-dependent Schrödinger equation for the one- and two-electron linear molecular ions H_3^{2+}, H_3^{+}, H_4^{3+}, H_4^{2+}, H_5^{4+}, and H_5^{3+} at fixed internuclear distance and parallel to the laser polarization have been obtained in intense laser pulses ($I \geq 10^{14}$ W/cm^2) in order to examine the effect of electron-electron interactions on high-order harmonic generation in extended (delocalized) systems. It is found that, in general, two-electron effects produce longer plateaus at large internuclear distances, thus enhancing harmonic generation well beyond the I_p+3U_p atomic maximum order cutoff law, where I_p is the ionization potential and U_p the ponderomotive energy. A second plateau is usually found at critical distances $R_c = (\pi/2)\alpha_0$ with a cutoff at energy I_p+6U_p in one-electron systems and I_p+12U_p for two-electron systems, where α_0 is the ponderomotive radius. Initial delocalized states, such as molecular orbitals, are shown to create longer harmonic generation plateaus and one can therefore attribute enhancement of harmonic generation plateaus by electron repulsion due to the increased separation and delocalization of electrons in extended systems by correlation effects. [S1050-2947(99)02501-9]

PACS number(s): 42.50.Vk

I. INTRODUCTION

Experimental and theoretical studies on the properties of atoms in intense laser pulses have led to the discovery of highly nonperturbative, nonlinear optical phenomena such as above threshold ionization and high-order harmonic generation (HG) [1]. The investigation of such nonperturbative phenomena in molecules is currently being pursued with the motivation that the extra degree of freedom due to nuclear motions can produce effects such as above threshold dissociation, laser-induced avoided crossing of potential surfaces [2], and the recently discovered phenomenon of charge resonance enhanced ionization at large internuclear distances [3–10]. The latter ionization enhancement also produces enhanced HG in molecular ions as has been shown in exact numerical simulations of one-electron molecular ions H_2^{+} [3]. The enhancement of ionization of molecular ions by short intense laser pulses has also been shown to persist in the presence of two-electron Coulomb repulsive effects [11] with little effect on the critical distance R_c, where such nonperturbative laser-induced effects are expected to occur.

Numerical simulations of the time-dependent Schrödinger equation (TDSE) for two-electron atoms [12–14] have focused on the problem of direct versus stepwise ionization. A recollision model of an electron with the core ion for explaining high-order HG [15,16] has been invoked as a possible mechanism for enhanced ionization of atomic systems [17,18]. Previous calculations of HG in one-dimensional negative ions have concluded that the inner electron can be passive or active as the laser field is weak or strong [12,13,19].

In the present work we extend our previous numerical solutions of the TDSE of one-electron and two-electron molecular systems to examine the effect of electron-electron repulsion and hence correlation on high-order HG in such systems. As previously shown in our work on one-dimensional models of H_2 and H_3^{+} [11], the electron correlation produces initial electron states with electrons well separated in space, but the antisymmetry of the initial two-electron wave function ensures a highly coherent delocalized state. Thus, in extended systems such as molecules, recollision of electrons with different nuclear sites induced by intense laser pulses has no counterpart in the simpler atomic systems. Thus, in one-electron extended molecular systems such collision of electrons with neighboring ions produces high-order HG [20,21] well beyond the established atomic I_P+3U_p cutoff law [15,16], where I_p is the ionization potential and U_p the ponderomotive energy. Thus cutoffs at I_P+6U_p and I_P+8U_p in the HG spectrum have been predicted to occur at large internuclear distances. In the present work we examine the effect of electron correlation in the one-dimensional two-electron models H_3^{+}, H_4^{2+}, and H_5^{3+} on these new cutoff laws. It is expected that such recollision effects should dominate in high-order HG by clusters subjected to short intense laser pulses [22–25].

II. ONE-ELECTRON SIMPLE MODELS

Exact numerical solutions of the TDSE for the one-electron H_2^{+} molecular ion produced a HG spectrum with two distinct plateaus: one short plateau of molecular origin and the other long one due to the ionized electron [3]. We present first two simple one-electron models that will help us understand the results to follow for the larger extended H_3^{+} and H_5^{3+} systems.

A. Essential two-state quantum model

Symmetric molecular ions such as H_2^{+} differ from atoms in that single valence electrons occupy molecular orbitals that are degenerate upon dissociation of the ion. Such degeneracy results in electronic transition moments that diverge as $R/2$, one-half the internuclear distance, due to charge reso-

nance (CR) effects [2,26]. This leads readily to nonperturbative molecule-field interactions as the ion dissociates [2]. Taking H_2^+ as our example, the CR radiative couplings are limited to the ground $1\sigma_g$ and first excited $1\sigma_u$ electronic states that dissociate into $H(1s)+H^+$ and are well separated from other excited states at large distances. These two first states are the doorway or essential electronic states for the ionization process. Thus (see, e.g., Fig. 11 in Ref. [27]) the two-state molecule-field Hamiltonian $H(t)$ coupling the $1\sigma_g$ and $1\sigma_u$ molecular orbitals can be reexpressed in terms of the localized left $|1\rangle=1s_a=(1\sigma_g+1\sigma_u)/\sqrt{2}$ and right $|2\rangle=1s_b=(1\sigma_u-1\sigma_g)/\sqrt{2}$ H atom orbitals

$$H(t)=\Omega\cos(\omega t)(|1\rangle\langle 1|-|2\rangle\langle 2|)+\Delta(|1\rangle\langle 2|+|2\rangle\langle 1|), \tag{1}$$

where Ω is the Rabi frequency $\Omega=\mathcal{E}_0R/2$, $\mathcal{E}_0$ is the field amplitude, and 2Δ is the electronic energy separation $2\Delta=[\epsilon_u(R)-\epsilon_g(R)]$. The general solution can be expressed as

$$\Psi(t)=C_1(t)\exp\left[-i\left(\frac{\Omega}{\omega}\right)\sin(\omega t)\right]|1\rangle + C_2(t)\exp\left[i\left(\frac{\Omega}{\omega}\right)\sin(\omega t)\right]|2\rangle \tag{2}$$

yielding equations for the amplitudes $C(t)$ from the Schrödinger equation

$$\frac{idC_1(t)}{dt}=\Delta\exp\left[i\left(\frac{2\Omega}{\omega}\right)\sin(\omega t)\right]C_2(t),$$
$$\frac{idC_2(t)}{dt}=\Delta\exp\left[-i\left(\frac{2\Omega}{\omega}\right)\sin(\omega t)\right]C_1(t). \tag{3}$$

For visible light energies, e.g., at 800 nm, $\omega\simeq 1.5$ eV and at large internuclear distances $R>6$ a.u. where $\Delta\ll\omega$, to lowest order of Δ/ω, one can reexpress Eq. (3) as

$$\frac{idC_1}{dt}=\Delta J_0\left(\frac{2\Omega}{\omega}\right)C_2(t),\quad \frac{idC_2}{dt}=\Delta J_0\left(\frac{2\Omega}{\omega}\right)C_1(t), \tag{4}$$

where

$$J_0\left(\frac{2\Omega}{\omega}\right)=\frac{\omega}{2\pi}\int_0^{2\pi/\omega}\exp\left[\frac{2i\Omega}{\omega}\sin(\omega t)\right]dt \tag{5}$$

is the zeroth-order Bessel function. Thus the transition probability between the localized atomic states $|1\rangle$ and $|2\rangle$, $P_{12}(t)$, is readily given from Eq. (4) as

$$P_{12}(t)=\sin^2\left[J_0\left(\frac{2\Omega}{\omega}\right)\Delta t\right]. \tag{6}$$

Such a result has been anticipated previously for two-level excitations [28] and has been discussed in the problem of tunneling suppression by periodic fields [29,30]. As noted by these previous authors, the effective tunneling between states $|1\rangle$ and $|2\rangle$ if one considers Eq. (1) as a tunneling Hamiltonian is reduced by the factor $J_0(2\Omega/\omega)$ and vanishes at the special condition

$$J_0\left(\frac{2\Omega}{\omega}\right)=0. \tag{7}$$

Such laser-induced tunneling suppression has been shown to exist in H_2^+ and can be interpreted as laser-induced localization [3,6,27].

The general case where $\Omega>\Delta,\omega$ can be considered as a time-dependent nonadiabatic transition problem between the two adiabatic surfaces $\pm(\Delta^2+\Omega^2\cos^2\omega t)^{1/2}$ and has been treated in detail by Kayanuma [31]. Assuming well-localized transitions around times $t_n=(n-\frac{1}{2})\pi/\omega$ $(n=1,2,\ldots)$, P_n, the probability that the system is in state $|2\rangle$ after the nth crossing, is essentially the Landau-Zener transition probability

$$P_n\sim e^{-2\pi\delta},\quad \delta=\Delta^2/2\Omega\omega. \tag{8}$$

This simple two-state model therefore predicts laser-induced localization [3,6] and laser-induced nonadiabatic transitions in the two-essential-state manifold $|1\rangle$ and $|2\rangle$. We shall be looking at extended systems with large internuclear distances where $\Delta<\Omega,\omega$. This corresponds to the diabatic regime where the essential doorway states are equally excited [27].

B. Classical electron model

One of the first models proposed to explain the emision of coherent radiation by electron scattering on a metallic surface is related to the Smith-Purcell effect [32,33]. In the present molecular context, the metal ion grating is replaced by the proton array or ''wire,'' H_3^{3+}, H_4^{4+}, and H_5^{5+}, to which we add one or two electrons. The interaction of free ionized electrons driven by the laser field $\mathcal{E}_0\cos(\omega t)$ (in a.u. $e=\hbar=m=1$) is described classically by the equation

$$\ddot{Z}(t)=-\mathcal{E}_0\cos(\omega t+\varphi),$$
$$\dot{Z}(t)=-(\mathcal{E}_0/\omega)[\sin(\omega t+\varphi)-\sin(\varphi)], \tag{9}$$
$$Z(t)=\alpha_0[\cos(\omega t+\varphi)+\omega t\sin(\varphi)-\cos(\varphi)], \tag{10}$$

where φ is the initial laser phase at which the electron is ionized and we assume an initial zero velocity $\dot{Z}(0)=0$. α_0 is the ponderomotive (quiver) radius in a.u. and U_p is the corresponding ponderomotive energy

$$\alpha_0=\mathcal{E}_0/\omega^2,\quad U_p=\frac{1}{4}\alpha_0^2\omega^2=\mathcal{E}_0^2/4\omega^2. \tag{11}$$

The classical equations (9) and (10) allow us to predict the optimal conditions for HG. As a first hypothesis we shall look at maximum acceleration, which in the classical limit should produce maximum radiation [34]. From Eq. (9) we obtain $\ddot{Z}(\max)$ at phase $\omega t+\varphi=\pi$. This yields the velocity $\dot{Z}=\mathcal{E}_0\sin(\varphi)/\omega$ with a maximum $\dot{Z}(\max)=\mathcal{E}_0/\omega$ for $\varphi=\pi/2$. The resulting energy is

$$E(\max)=\frac{\dot{Z}^2}{2}=\frac{\mathcal{E}_0^2}{2\omega^2}=2U_p. \tag{12}$$

The corresponding minimum distance required by the electron to collide with a neighboring ion is then obtained from Eq. (10) as

$$Z(t)=\alpha_0[-1+\omega t]=\alpha_0[\pi/2-1]=0.57\alpha_0. \quad (13)$$

Thus the maximum acceleration criterion yields a maximum harmonic order $N_m=2U_p/\omega$ at an internuclear distance $R=0.57\alpha_0$ during a quarter cycle $t=\pi/2\omega$.

The next scenario is the recombination of the electron with the parent ion [20,21]. For maximum velocity, the phase requirement is $\omega t+\varphi=3\pi/2$, thus yielding the transcendental equation $(3\pi/2-\varphi)\sin(\varphi)=\cos(\varphi)$, the solution of which is $\varphi=0.08\pi$, $\dot{Z}(\max)=1.26\mathcal{E}_0/\omega$. The resulting maximum energy is

$$E(\max)=3.17U_p. \quad (14)$$

This simple classical model explains the theoretical order cutoff law for HG in atoms by recollision [15,16]

$$N_m=(I_p+3.17U_p)/\omega, \quad (15)$$

where I_p is the ionization potential. However, in the molecular case, collisions will occur with neighboring ions as in Eq. (13). Then the maximum velocity condition $\omega t+\varphi=3\pi/2$ gives this velocity from Eq. (9) to be $\dot{Z}=(8\mathcal{E}_0/\omega)[1+\sin(\varphi)]$, i.e., $\dot{Z}(\max)=2\mathcal{E}_0/\omega$ at $\varphi=\pi/2$. Thus the maximum energy obtained with no constraints is

$$E(\max)=\frac{2\mathcal{E}_0^2}{\omega^2}=8U_p. \quad (16)$$

This is gained during *half* a cycle since $\omega t=\pi$. The corresponding minimum distance traveled by the electron is from Eq. (10)

$$Z(\pi/\omega)=\pi\alpha_0. \quad (17)$$

In summary, one sees from the above simple classical model that collisions with neighboring ions can lead to a larger HG spectrum with a cutoff up to the maximum harmonic N_m given by

$$N_m\simeq(I_p+8U_p)/\omega. \quad (18)$$

This larger extended cut-off law involving collisions with neighboring ions requires an initial laser phase $\varphi=\pi/2$, i.e., $\mathcal{E}(t)=\mathcal{E}_0\sin(\omega t)$ with $\mathcal{E}(0)\simeq 0$. Thus, in this more extended HG spectrum, unfortunately little ionization occurs initially and we have suggested that a two-laser scheme is required to render such molecular HG more efficient [20]. Setting next $Z(t)=\pi\alpha_0/2$, yields after simple calculation another cutoff law $N_m\simeq(I_p+6U_p)/\omega$ with $\varphi=\pi/2$ and $\omega t=3\pi/4$, which was confirmed numerically for one-electron systems H_2^+ and H_3^{2+} [20]. In conclusion, the classical model (9) and (10) predicts maximum kinetic energies $2U_p$, $6U_p$, and $8U_p$ by collision with neighboring ions at the minimum distances $(\pi/2-1)\alpha_0$ at time $t=\pi/2\omega$, $(\pi/2)\alpha_0$ at $t=3\pi/4\omega$, and $\pi\alpha_0$ at $t=\pi/\omega$. Assuming further that the initial velocity is nonzero, i.e., $\dot{Z}(0)=v_0\neq 0$, one can in principle obtain harmonics beyond the $8U_p$ law [20,21].

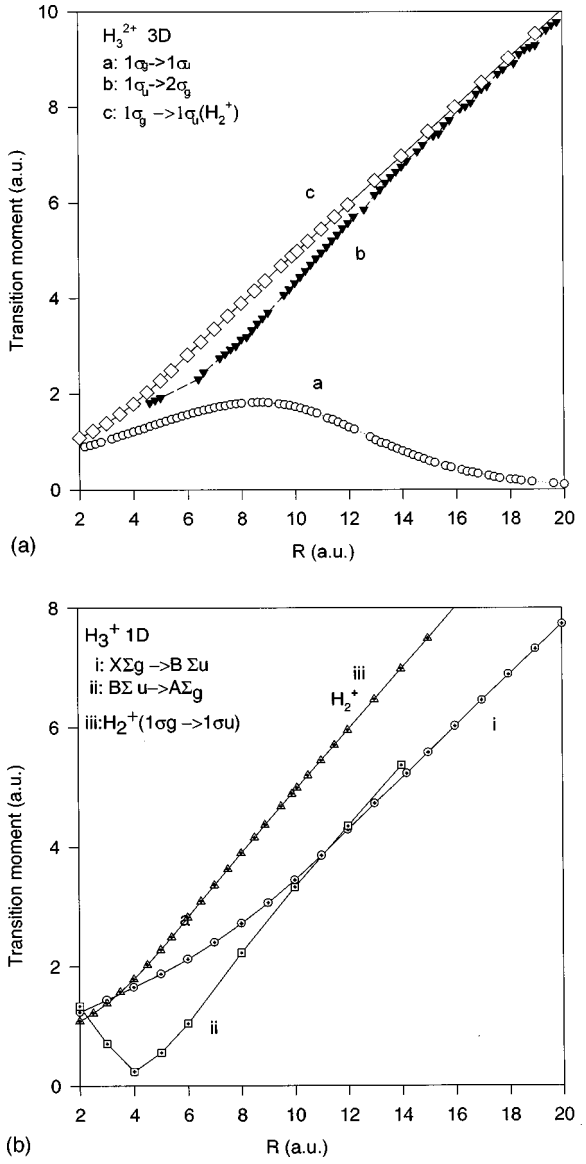

FIG. 1. Electronic transition moments as a function of total R for (a) H_3^{2+} (three dimensions): a, $1\sigma_g\rightarrow 1\sigma_u$; b, $1\sigma_u\rightarrow 2\sigma_g$; and c, H_2^+, $1\sigma_g\rightarrow 1\sigma_u$; and for (b) H_3^+ (one dimension): i, $X\Sigma_g\rightarrow B\Sigma_u$; ii, $B\Sigma_u\rightarrow A\Sigma_g$; and iii, H_2^+, $1\sigma_g\rightarrow 1\sigma_u$.

III. NUMERICAL METHOD

We have solved the TDSE for both one-electron linear systems H_3^{2+}, H_4^{3+}, and H_5^{4+} parallel with and interacting with intense laser pulses using an exact three-dimensional (3D) Hamiltonian and a 1D Hamiltonian with a regularized (softened) Coulomb potential to remove singularities in the two-electron systems. Descriptions of both methods can be found in earlier references [11,27]. We present here briefly the method for the 3D model. Thus, for the H_3^{2+} molecular ion, the laser-molecule TDSE is written in a.u. as

$$i\frac{\partial}{\partial t}\Psi(\rho,Z,R,t)=[H_0(\rho,Z,R,t)+V_n+V_{ext}]\Psi(\rho,Z,R,t), \quad (19)$$

where

$$H_0(\rho,Z,R,t)=-\frac{1}{2}\frac{\partial^2}{\partial^2 Z}-\frac{1}{2}\left(\frac{1}{\rho}\frac{\partial}{\partial\rho}+\frac{\partial^2}{\partial^2\rho}\right),$$

$$V_n=-\left[\rho^2+\left(Z-\frac{R}{2}\right)^2\right]^{-1/2}-\left[\rho^2+\left(Z+\frac{R}{2}\right)^2\right]^{-1/2}$$
$$-[\rho^2+Z^2]^{-1/2}, \tag{20}$$

$$V_{ext}=-\mathcal{E}_0 Z\cos(\omega t).$$

V_n is the total electron-nucleus Coulomb attraction potential, R is the internuclear distance and laser polarization axis, and ω and $\mathcal{E}_0$ are the laser frequency and amplitude, respectively. $\rho=(x^2+y^2)^{1/2}$ is the electron cylindrical coordinate since we assume that the field is parallel to the Z (electron) and R (molecular) axis. Thus, in cylindral coordinates, the electronic problem is reduced to two dimensions for fixed nuclei, whereas for moving nuclei, it is a real 3D problem [10]. $Z=0$ is the center of the molecule. The wave function $\Psi(\rho,Z,R,t)$ in Eq. (19) is advanced in a time step δt by an exponential method

$$\Psi(\rho,Z,R,t)=-\exp\left(-\frac{i}{2}\delta t H_0\right)\exp[-i\,\delta t(V_n+V_{ext})]$$
$$\times\exp\left(-\frac{i}{2}\delta t H_0\right)+O(\delta t^3). \tag{21}$$

Singularities in the Coulomb potential V_n and the kinetic-energy Hamiltonian H_0 are removed either by expanding in Bessel functions and propagating then with a high-level split-operator method [35] or by using a Crank-Nicholson scheme [27]. The corresponding linear 1D Hamiltonian for H_3^+ can be found in our recent work [11]. Calculations are performed for various fixed proton distances R, with the laser field parallel to the molecular ion axis. The grid size for such calculations is governed by the dimension of the ponderomotive radius $\alpha_0=\mathcal{E}_0/\omega^2$, so that in general $Z=\pm 630$ a.u. (2520 grid points) and $\rho=32$ a.u. (128 grid points). The step sizes in Z and t are determined by the limits imposed by the uncertainty principle $\delta Z\,\delta p=\delta E\,\delta t\simeq 1$ [e.g., for $E(\max)=5$ a.u., $p(\max)=\sqrt{10}$ a.u., $\delta x\leqslant 0.3$ a.u., and $\delta t\leqslant 0.2$ a.u.]. An absorbing potential is used at both Z and ρ boundaries. The ionization rate Γ (s^{-1}) is then obtained as the time decrease of the norm $dN/dt=-\Gamma N$, $N=\int|\Psi|^2 dv$.

HG spectra are obtained from the power spectrum of the laser-molecule system in conformity with the classical model of a radiating dipole [34]. Thus one calculates the field-induced dipole moment in the length gauge

$$Z(t)=\langle\Psi(\rho,Z,R,t)|Z|\Psi(\rho,Z,R,t)\rangle \tag{22}$$

or the equivalent acceleration $\ddot{Z}(t)$ expression [36,37], which is then Fourier transformed to give $Z(\omega)$. The power or HG spectrum is reported here as $|Z(\omega)|^2$, which agrees with the acceleration results except for a larger background due to the permanent field-induced moments [36]. These are single-particle spectra that neglect the interparticle coherences created by an intense nonperturbative field [38]. All HG spectra reported here have been calculated under the same pulse con-

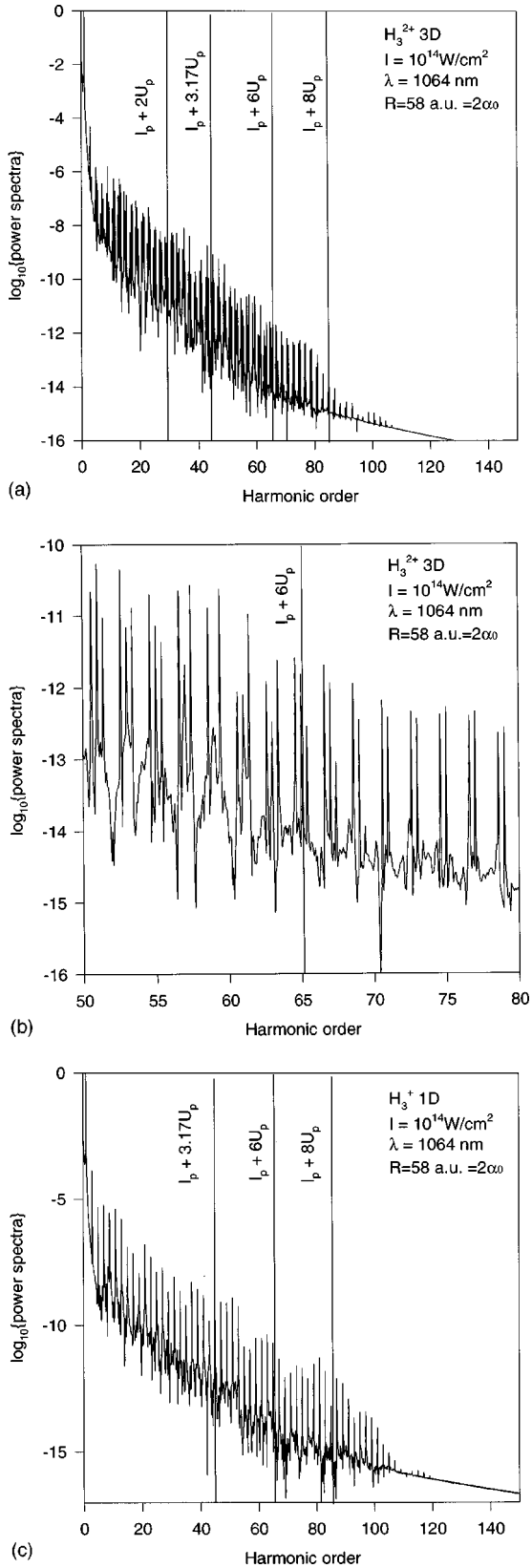

FIG. 2. Harmonic generation spectra at $I=10^{14}$ W/cm^2. $\lambda=1064$ nm, $R=R_{12}+R_{23}=58$ a.u.$=2\alpha_0$ for (a) H_3^{2+} (three dimensions), (b) H_3^{2+} (three dimensions), and (c) H_3^+ (one dimension).

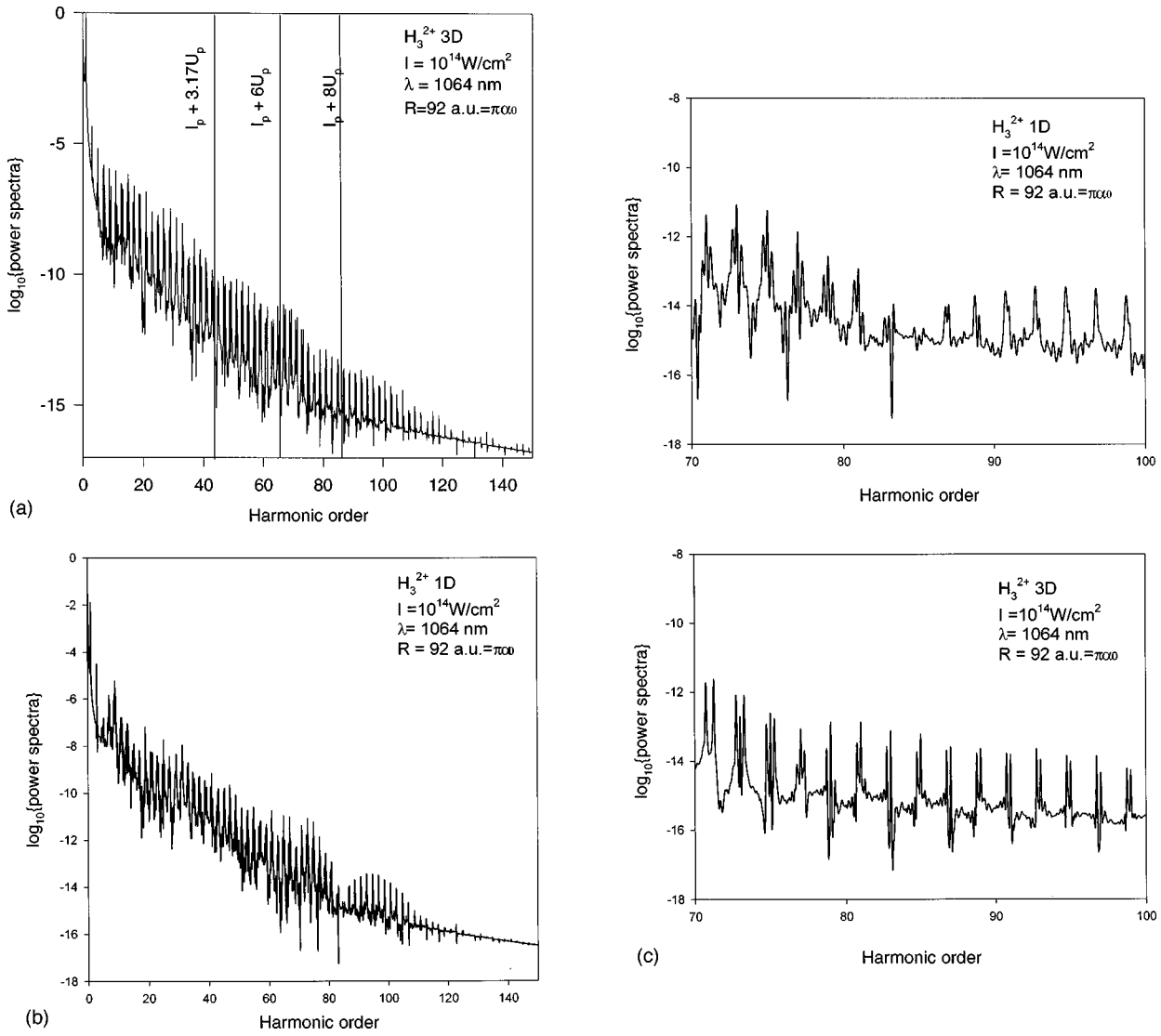

FIG. 3. Harmonic generation spectra at $I=10^{14}$ W/cm^2. $\lambda=1064$ nm for (a) H_3^{2+} (three dimensions), $R=R_{12}+R_{23}=92$ a.u. $=\pi\alpha_0$; (b) H_3^{2+} (one dimension), $R=\pi\alpha_0$; (c) H_3^{2+} (one dimension) and H_3^{2+} (three dimensions), $R=\pi\alpha_0$; (d) H^+-H(1s)-H^+, $R=92$ a.u.; (e) H_3^+ (one dimension), $R=92$ a.u.; (f) H_2($R_e=2$ a.u.)-H^+, $R=46$ a.u.$=\pi\alpha_0/2$; and (g) H_2($R_e=2$ a.u.)-H^+, $R=92$ a.u.$=\pi\alpha_0$.

ditions: a 5-cycle linear rise to the field amplitude $\mathcal{E}_0$, which is then maintained constant for 20 cycles.

IV. H_3^{2+} AND H_3^+ HARMONIC GENERATION SPECTRA

As pointed out in Sec. II, HG is expected to have plateaus that exceed the $(I_p+3.17U_p)/\omega$ maximum harmonic order N_m [Eq. (15)] at large internuclear distances R where the lowest electronic energy separation 2Δ is much less than the laser frequency ω and the Rabi frequency Ω. Thus for symmetric systems such as H_2^+, H_3^{2+} and H_3^+, the first two (H_2^+) and three (H_3^{2+} and H_3^+) electronic states are the doorway or essential states for the nonperturbative nonlinear optical properties of these systems as they are highly populated by the intense field according to Eq. (8). To illustrate therefore the difference between the one- and two-electron doorway state systems, we report in Fig. 1(a) the first two electronic transition moments of H_3^{2+} and in Fig. 1(b) the corresponding transition moments in H_3^+ with that of H_2^+ for comparison. Thus, in the case of H_3^{2+} at short distance the (a) $1\sigma_g\rightarrow 1\sigma_u$ and (b) $1\sigma_u\rightarrow 2\sigma_g$ moments behave as $R/2\sqrt{2}$, corresponding to transitions between highly delocalized orbitals: $(1/\sqrt{2})[1s_2\pm(1/\sqrt{2})(1s_1+1s_3)]$ for the g orbitals and $(1/\sqrt{2})(1s_1-1s_3)$ for the u orbital where $1s_i$ is the 1s atomic orbital on proton i [39]. At large distances, the ground $1\sigma_g$ molecular orbital correlates to the central atomic $1s_2$ orbital as the molecular ion dissociates to H^+-H-H^+. The $1\sigma_u$ and $2\sigma_g$ orbitals then become essentially $(1/\sqrt{2})[1s_1\pm 1s_3]$ with the corresponding transition moment $R/2$ as for H_2^+. This asymptotic behavior is clearly evident in Fig. 1(a).

The behavior of these transition moments for H_3^+ [Fig. 1(b)], illustrates the effect of the electron correlation on the dissociation of the latter. Thus, whereas H_3^{2+} dissociates into $H^+H(1s)H^+$, H_3^+ decomposes into $H(1s)H^+H(1s)$ with the electrons well separated at all times. This electron repulsion effect can also be seen clearly in the electron density for H_3^+ illustrated in Fig. 1 of Ref. [11]. Thus, accord-

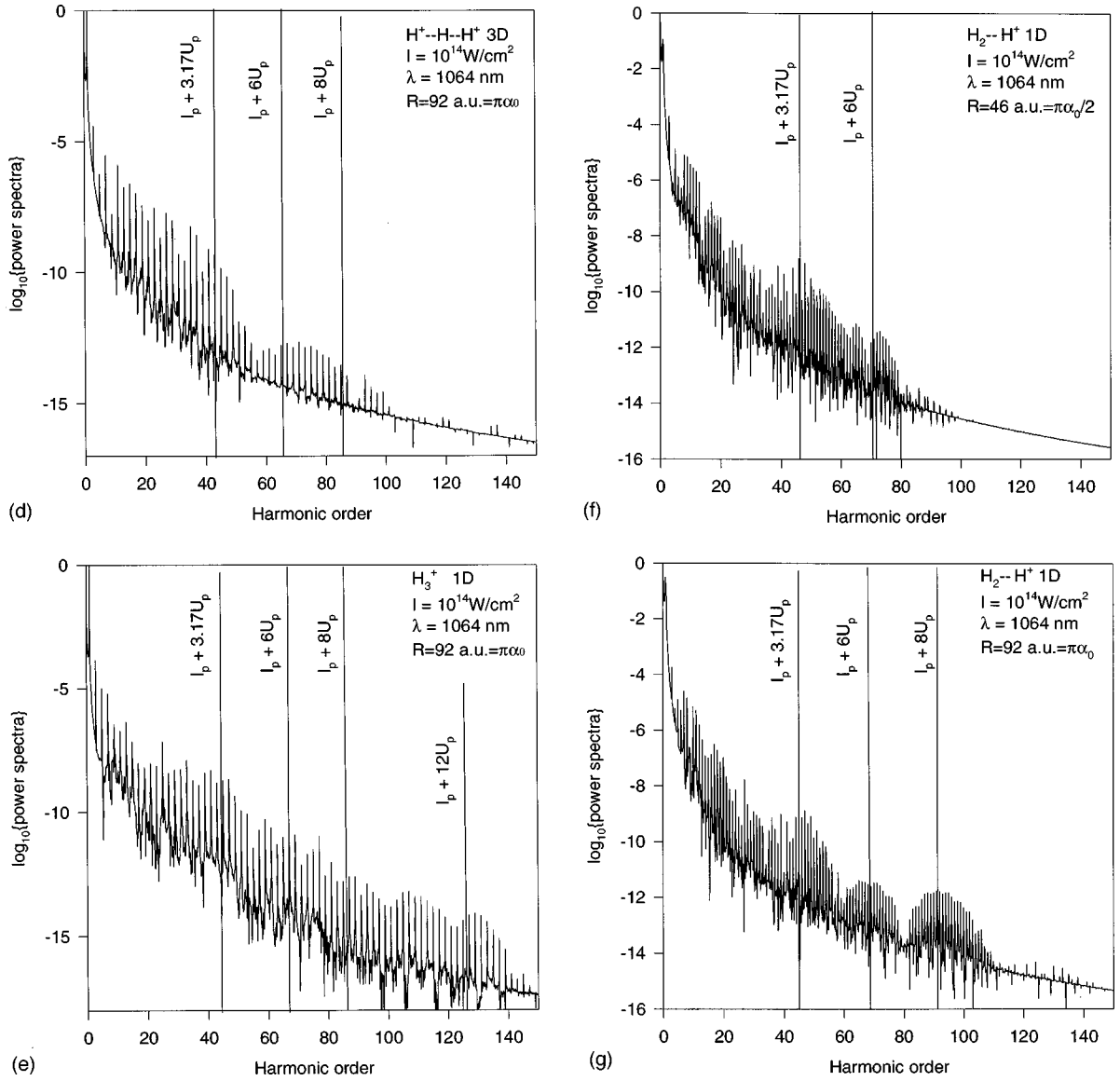

FIG. 3. (*Continued*).

ing to the present Fig. 1(b), the two first transition moments in H_3^+ behave as $R/2\sqrt{2}$ (curves *i* and *ii*) as compared to $R/2$ in H_2^+ (curve *iii*). The symmetry of the two-electron wave function in addition to the Coulomb repulsion maintains delocalization of the two electrons at both ends of the molecule in H_3^+ in all three electronic states, whereas in H_3^{2+} the single electron becomes localized in the ground $1\sigma_g$ state and because of orthogonality is delocalized at both ends of the molecule only in the two excited states $1\sigma_u$ and $2\sigma_g$.

For the laser conditions $I=10^{14}$ W/cm$^2 \simeq 2.85 \times 10^{-3}$ a.u., $\lambda = 1064$ nm, and $\omega = 0.0428$ a.u., one obtains the following laser electron parameters employed in Sec. II: the ponderomotive radius $\alpha_0 = 29$ a.u., $\pi\alpha_0/2 = 46$ a.u., and $\pi\alpha_0 = 92$ a.u. The ponderomotive energy $U_p = 0.388$ a.u. $= 9\omega$. At large distances, I_p for H_3^+ and H_3^{2+} is essentially $I_p(\mathrm{H}) = 0.5$ a.u. $= 12\omega$. One expects therefore a HG cutoff at the maximum harmonic $N_m \simeq (I_p + 3.17U_p)/\omega = 41$. The $(I_p + 6U_p)/\omega$ law would give $N_m \simeq 67$ and $(I_p + 87U_p)/\omega$ would correspond to $N_m \simeq 85$.

In Fig. 2 we illustrate the HG spectrum for H_3^{2+} [Figs. 2(a) and 2(b)] and H_3^+ [Fig. 2(c)] at the total internuclear distance $R = R_{12} + R_{13} = 58$ a.u. $= 2\alpha_0$. This distance was chosen in order to make the ponderomotive turning points $\pm\alpha_0$ of an ionized electron to coincide with the fixed proton positions $R_{12} = R_{23} = R/2 = \alpha_0$. At such turning points, the electron velocity would be zero with therefore little kinetic energy. Figure 2(a) shows clearly the extension of the $I_p + 3.17U_p$ plateau beyond $6U_p$. Of note is the triple structure of each harmonic. Such a triplet structure is predicted for a two-level system [3,27,40–42] under the influence of an intense laser field when the energy separation $\Delta \ll \omega$, as discussed in Sec. II A, Eq. (6). In the case of H_3^{2+}, the strongest radiative coupling occurs between the two excited states $1\sigma_u$ and $2\sigma_g$ that have an $R/2$ divergent transition moment [Fig. 1(b)]. Thus the HG spectrum [Fig. 2(a)] confirms that H_3^{2+} at large distances behaves as a two-level system, but, contrary to H_2^+ [3], the essential states are the first and second excited states. In Fig. 2(b) we have amplified the triplet structure. It is to be noted that after the $I_p + 6U_p$ cutoff at $N_m \simeq 65-67$, the triplet structure reduces to a doublet structure. Since the triplet HG spectrum is indicative of persistent molecular structure, the vanishing of the molecular influence

on the HG spectrum in the region of the cutoff seems to correlate with the free-electron nature of the highly nonlinear photophysical processes in the cutoff energy region. At the moment there is no adequate theoretical explanation for this phenomenon.

Figure 2(c) illustrates the HG spectrum of the two-electron H_3^+ under the same conditions as the one-electron H_3^{2+} [Figs. 2(a) and 2(b)]. We note first the absence of any triplet structure. This is consistent with the transition moments of H_3^+ [Fig. 1(b)], which show that due to electron repulsion, electron delocalization in all three essential states $1\sigma_g$, $1\sigma_u$, and $2\sigma_g$ results in nearly equal transition moments, so that now three essential states need to be considered and the triplet splitting characteristic of two-level systems is no longer operative. Second the $8U_p$ cutoff is now much more pronounced than in the single-electron case H_3^{2+} [Fig. 2(a)]. The net result of electron repulsion is a slight extension of the HG spectrum by about 10–15 % for $R=2\alpha_0$.

We next illustrate the HG spectrum at the total internuclear distance $R=R_{12}+R_{23}=92$ a.u.$=\pi\alpha_0/2$ for H_3^{2+} [Fig. 3[4](a)] in three dimensions, Figs. 3(b) and 3(c) in one dimension, H^+-H($1s$)-H^+ in three dimensions [Fig. 3(d)] and H_3^+ in one dimension [Fig. 3(e)]. Figures 3(a), 3(b), and 3(e) correspond to exact, completely *delocalized* initial states obtained by propagating the middle $1s_2$ H atom in imaginary time [11]. Figure 3(d) corresponds to an initial $1s_2$ H orbital, i.e., a completely *localized* initial state. The exact single-electron H_3^{2+} case [Fig. 3(a)] shows a less well separated triplet structure than in Fig. 2(a) and a longer HG spectrum than in Fig. 3(d), the initial localized atomic state case. Figure 3(b) shows the same calculation as in Fig. 3(a), the 3D case at $R=\pi\alpha_0$, but now in one dimension. A strong dip is observed at $8U_p$ energy for the 1D case. The I_p+6U_p maximum seems to be the same in both one and three dimensions, thus lending confidence to the results of Sec. V for large systems. Figure 3(c) shows the detailed structure of the 1D and 3D HG system of H_3^{2+} between orders 70 and 100. In the both cases, triplet Rabi splittings occur below energies I_p+6U_p, which then become doublets for harmonics above that energy. This phenomenon was also observed at $R=2\alpha_0$ (Fig. 2) and is an intriguing new property of HG spectra in delocalized systems.

The $6U_p$ maximum or cutoff appears clearly in Figs. 3(a)–3(c), in agreement with the prediction in Sec. II B that an electron encounters a proton at R = $\pi\alpha_0/2$ with maximum kinetic energy of $6U_p$. The $6U_p$ maximum also appears in the initially localized electron case [Fig. 3(d)], but with a lower efficiency of about one order of magnitude.The latter shows no splitting of the harmonics. Figures 3(a) and 3(d) show clearly the reduction in the HG spectrum length and efficiency whenever the initial electron is localized rather than delocalized. Figure 3(e) shows the two-electron H_3^+ system under the same excitation conditions. One sees now a dramatic change, a near *doubling* of the HG spectrum as compared to the single-electron case. Again there is no splitting of harmonics in the two-electron case. There is an apparent cutoff at $12U_p$. We add for comparison a nonsymmetric case H_2-H^+, where the two electrons are now initially localized in an equilibrium H_2 molecule ($R_e=2$ a.u.) and are accelerated by the laser field towards a proton at distance

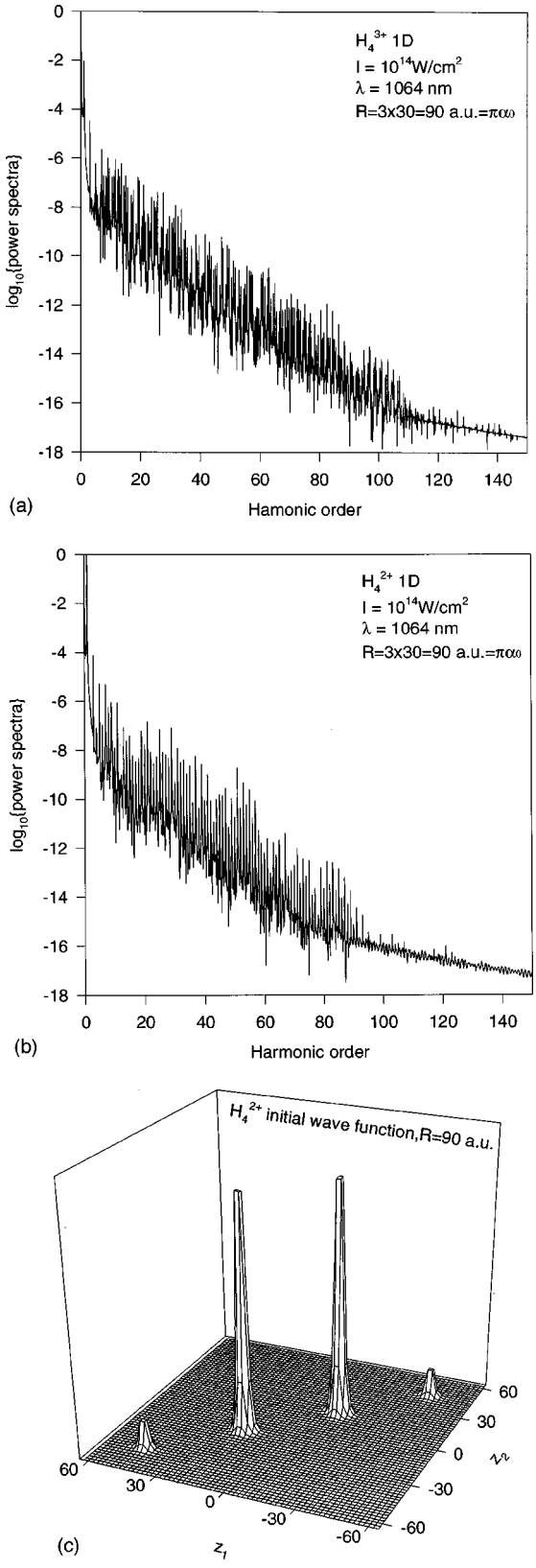

FIG. 4. Harmonic generation spectra at $I=10^{14}$ W/cm^2. $\lambda=1064$ nm for (a) equal bond H_4^{3+} (one dimension), $R=3R_{\mathrm{HH}}=90$ a.u.$=\pi\alpha_0$; (b) H_4^{2+} (one dimension), $R=3R_{\mathrm{HH}}=90$ a.u. $=\pi\alpha_0$; and (c) H_4^{2+} (one dimension) initial electron wave function with electronic coordinates Z_1, Z_2.

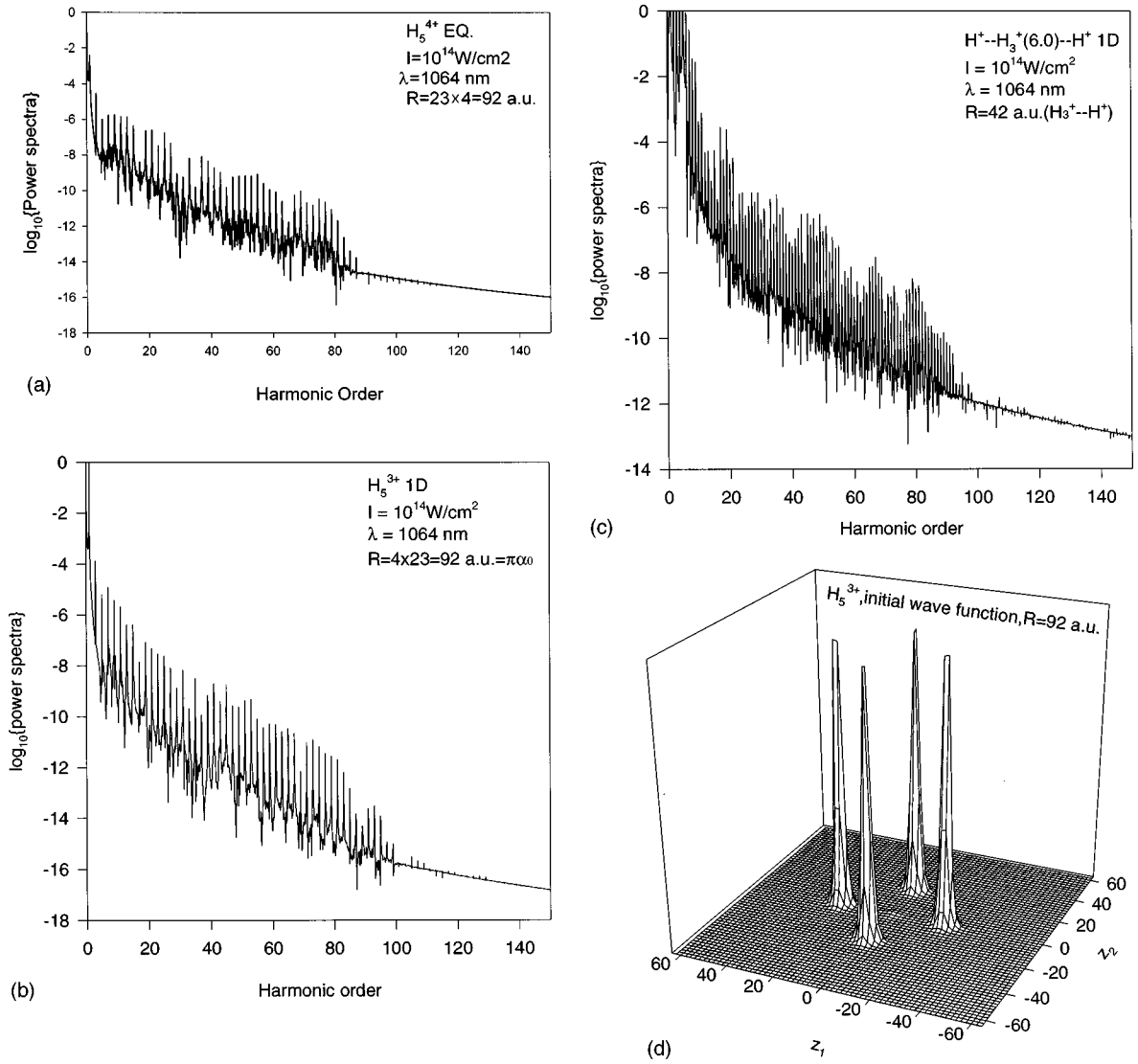

FIG. 5. Harmonic generation spectra at $I=10^{14}$ W/cm^2. $\lambda=1064$ nm for (a) equal bond H_5^{4+} (one dimension), $R=4R_{HH}=92$ a.u. $=\pi\alpha_0$; (b) H_5^{3+} (one dimension), $R=4R_{HH}=92$ a.u. ; (c) H^+-H_3^+-H^+ (one dimension), $R=42+6+42=90$ a.u.; and (d) a two-electron wave function for equidistant H_5^{3+} (one dimension). Z_1,Z_2 are electron coordinates.

$R=\pi\alpha_0/2$ [Fig. 3(f)] and $\pi\alpha_0$ [Fig. 3(g)]. Thus, as in H_3^{2+}, the maximum cutoff appears around $6U_p$, which corresponds to $N_m\simeq 70$ for H_2-H^+ due to the larger I_p of H_2 (0.81 vs 0.5 a.u.). Following the classical electron model Sec. II B, electrons situated at distances $\pi\alpha_0/2$ from a neighboring proton will collide with this neighbor with kinetic energy around $6U_p$. This is consistent with the HG spectra of H_3^{2+} [Figs. 3(a)–3(d)] and H_2-H^+ [Fig. 3(f)]. In the first case, the electron is initially concentrated on the middle proton and thus collides with the outer protons at a distance $R_{12}=R_{23}=\pi\alpha_0/2$, thus generating harmonics up to order $N_m\simeq I_p+6U_p$. In the nonsymmetric H_2-H^+ initial case [Fig. 3(f)] both electrons are now initially at a distance $R=\pi\alpha_0/2$ from the external proton, with therefore the same plateau as in the H_3^{2+} case, except for the appearance of even harmonics in the nonsymmetric initial state. The highly symmetric H_3^+ case corresponds basically to two electrons separated at each end of the molecule by electron repulsion at a distance $R=\pi\alpha_0$. Under the influence of the intense laser field, both electrons can move in phase, in and out of the molecular region. In doing so each electron will collide initially with the central proton at $R_{12}(R_{23})=\pi\alpha_0/2$ and finally with the external proton situated at $R=\pi\alpha_0$. Both collisions should release energies I_p+6U_p and I_p+8U_p according to the independent-electron model [Eqs. (9) and (10) and also Fig. 3(e)]. The extension of the HG spectrum up to I_p+12U_p, in H_3^+, beyond the I_p+8U_p single-electron law could be ascribed to a coherent two-electron correlation effect. We emphasize that two initially localized electrons as in H_2 [Fig. 3(g)] give only a I_p+8U_p cutoff, whereas two electrons completely delocalized in the symmetric H_3^+ [Fig. 3(e)] give harmonics of order up to $N_m=(I_p+12U_p)/\omega$. This suggests that in the middle of the molecule, i.e., at $R=\pi\alpha_0/2$, one electron exchanges $6U_p$ of kinetic energy by a collision with the other, thus giving a maximum of $12U_p$ as observed in the H_3^+ system [Fig. 3(e)]. Previous simulations in the two-electron H_2 molecule shows frequent electron-electron collisions in the center of the molecule [see Fig. 8 of Ref. [11(a)]]. Since we are dealing with fixed nuclei, the present long plateau suggests an electron collision mechanism.

V. H_4^{3+}, H_4^{2+}, H_5^{4+}, AND H_5^{3+}

In the present section we examine a 1D ''quantum wire'' made up of four and five protons. Recent studies on clusters show that the average distance between nuclei varies from 6 to 8 a.u. [43], which also corresponds to the critical distance R_c for enhanced ionization in H_3^{2+}, H_3^{+} [11], H_4^{3+}, and H_4^{2+} systems [44]. In the present section we examine the nature of high-order HG for an extended quantum wire, i.e., at large internuclear distances where electron collisions with neighboring ions is a predominant mechanism. All calculations are 1D.

In Figs. 4(a) and 4(b) we show the HG spectra of the one-electron H_4^{3+} and two-electron H_4^{2+} equidistant proton systems, respectively ($R=3R_{\rm HH}$). We have chosen the wire length to be $R=90$ a.u.$=\pi\alpha_0$ as in Fig. 3 for the H_3^{2+} and H_3^{+} systems. The one-electron systems H_3^{2+} [Fig. 3(a)] and H_4^{3+} [Fig. 4(a)] show similar behavior splitting of the harmonics due to Rabi effects and cutoffs in the HG spectrum around I_p+8U_p, as expected for a system of dimension $\pi\alpha_0$ [Eqs. (17) and (18)]. A comparison of the two-electron systems, H_3^{+} [Fig. 3(e)] and H_4^{2+} [Fig. 4(b)] shows a fundamental difference. The H_4^{2+} system shows a cutoff at around I_p+8U_p instead of I_p+12U_p. This can be shown to be due to the difference in the initial two-electron wave functions. Whereas in H_3^{+} both electrons are preferentially localized at the ends of the molecule, at $\pm R/2=\pi\alpha_0/2$ (see [11]), in H_4^{2+} [see Fig. 4(c)], both electrons tend to localize on the inner two protons with a separation $R_{\rm HH}=30$ a.u. Thus, because of the restricted delocalization of the initial state in this case, the HG plateau is restricted to maximum electron and hence photon energies of I_p+8U_p only. We note again that the line splittings [Fig. 4(a)] disappear in the two-electron case [Fig. 4(b)]. We next show in Fig. 5 the five equidistant proton ($R=4R_{\rm HH}$) quantum wire HG spectra. In Fig. 5(a) the one-electron H_5^{4+} spectra show a cutoff at energies I_p+6U_p, somewhat shorter than the corresponding H_3^{2+} plateau [Fig. 3(a)]. The two-electron system H_5^{3+} [Fig. 5(b)] remains essentially the same as the one-electron H_5^{4+} case [Fig. 5(a)]. We also show for comparison the H^+-H_3^+-H^+ nonequidistant proton system with the H_3^{+} length $R=6$ a.u, [Fig. 5(c)]. The length of the plateaus are similar in all three cases H_3^{2+}, H_5^{4+}, and H^+-H_3^+-H^+. An analysis of the two-electron wave functions for the equidistant protons, with $R_{\rm HH}=23$ a.u. [Fig. 5(d)], shows that H_5^{3+} has the behaviors of a H_3^{+} system with total length $R=2R_{\rm HH}=46$ a.u.$=\pi\alpha_0/2$, for which one would expect maximum electron and hence proton energies to be I_p+6U_p. We conclude from these results that incomplete electron delocalization in H_4^{2+} and H_5^{3+} over the whole length of the quantum wire decreases the length of the HG plateau expected.

VI. CONCLUSION

We have examined in the present work the effect of the electron correlation in extended delocalized systems, in which laser-induced collisions of electrons with neighboring ions are expected to produce longer HG plateaus than in single atomic systems. In the one-electron systems H_3^{2+}, H_4^{3+}, and H_5^{4+}, HG cutoffs around I_p+6U_p are found to occur with efficiencies 10^{-2}, that of the atomic and short molecule HG cutoffs of I_p+3U_p. Two-electron effects increase these cutoffs to I_p+12U_p (see Fig. 3(e)] for electrons localized at the distance $R_c\simeq(\pi/2)\alpha_0$. An unusual observation is that one-electron HG spectra show Rabi triplet splittings for energies below I_p+6U_p and only doublet splittings above that energy. Furthermore, there splittings vanish completely in the two-electron HG system. We currently have no explanation for this phenemenon.

Delocalized electron states are shown to always produce longer plateaus. Since delocalization is enhanced by electron correlation, e.g., H_3^{+} vs H_3^{2+}, one can therefore attribute longer plateaus to the correlation and electron energy transfer. This makes larger molecular ions and clusters attractive candidates to observe long HG plateaus. Current experiments show that it is now possible to create ion clusters or ''crystals,'' comprised of ions confined at large distances [45,46]. Such systems where interion distances are $(\pi/2)\alpha_0$ should create plateaus from I_p+6U_p to I_p+12U_p, the first where there is no electron correlation, the latter where electron correlation is strong and therefore results in enhanced electron energy transfer. The present results were obtained with fixed nuclei, thus emphasizing electron-electron collision as a dominant mechanism for momentum transfer. Electron-nuclei momentum transfer can only be addressed in a full non-Born-Oppenheimer calculation, as recently done for the one-electron H_2^{+} case [10,47], and therefore remains a problem to be investigated.

ACKNOWLEDGMENTS

We thank the Natural Sciences and Engineering Research Council of Canada (NSERC) for their support of the present research and the Center d'Application de Calcul Parallèle (CACPUS) for access to an IBM-SP2 supercomputer.

[1] *Atoms in Intense Laser Fields*, edited by M. Gavrila (Academic, San Diego, 1992).
[2] A. D. Bandrauk, *Molecules in Laser Fields* (Dekker, New York, 1993), Chaps. 2–4.
[3] T. Zuo, S. Chelkowski, and A. D. Bandrauk, Phys. Rev. A **48**, 3837 (1993).
[4] A. D. Bandrauk, in *Resonance Ionization Spectroscopy and Its Applications 1996: Eight International Symposium*, edited by N. Winograd and J. E. Parks, AIP Conf. Proc. No. 388 (AIP, New York, 1996), p. 37.
[5] S. Chelkowski and A. D. Bandrauk, J. Phys. B **28**, L723 (1995).
[6] T. Zuo and A. D. Bandrauk, Phys. Rev. A **52**, R2511 (1995).
[7] E. Constant, H. Stapelfelt, and P. B. Corkum, Phys. Rev. Lett. **76**, 4140 (1996).
[8] T. Seidemanm, M. Ivanov, and P. B. Corkum, Phys. Rev. Lett. **75**, 2819 (1995).
[9] J. H. Posthumus, L. J. Frasinski, A. J. Giles, and K. Codling, J. Phys. B **28**, L349 (1995).
[10] S. Chelkowski, A. Conjusteau, T. Zuo, and A. D. Bandrauk,

Phys. Rev. A **52**, 2977 (1995); **54**, 3235 (1996).
[11] (a) H. Yu and A. D. Bandrauk, Phys. Rev. A **54**, 3290 (1996); (b) **56**, 685 (1997).
[12] R. Grobe and J. H. Eberly, Phys. Rev. Lett. **68**, 2905 (1992); Phys. Rev. A **47**, 1605 (1993); **48**, 4664 (1993).
[13] S. L. Haan, R. Grobe, and J. H. Eberly, Phys. Rev. A **50**, 378 (1994); **54**, 1576 (1996).
[14] D. Bauer, Phys. Rev. A **56**, 3028 (1997).
[15] J. L. Krause, K. J. Schafer, and K. C. Kulander, Phys. Rev. Lett. **68**, 3535 (1992).
[16] P. B. Corkum, Phys. Rev. Lett. **71**, 1994 (1993).
[17] J. B. Watson, A. Sanpera, D. G. Lappas, P. L. Knight, and K. Burnett, Phys. Rev. Lett. **78**, 1884 (1997).
[18] A. Becker and F. H. M. Faisal, J. Phys. B **29**, L1797 (1996).
[19] D. G. Lappas, R. Grobe, and J. H. Eberly, in *Proceedings of the VIth International Conference on Multiphoton Processes*, edited by S. L. Chin and D. K. Evans (World Scientific, Singapore, 1993), p. 369.
[20] A. D. Bandrauk, S. Chelkowski, H. Yu, and E. Constant, Phys. Rev. A **56**, 2537 (1997).
[21] P. Moreno, L. Playa, and L. Roso, J. Opt. Soc. Am. A **13**, 430 (1996); Phys. Rev. A **55**, 1593 (1997).
[22] T. D. Donnelly, T. Ditmire, K. Neuman, M. D. Perry, and R. W. Faleone, Phys. Rev. Lett. **76**, 2472 (1996).
[23] S. Dobosz, M. Lezius, M. Schmidt, M. Perdrix, D. Normand, J.-P. Rozet, and D. Vernhet, Phys. Rev. A **56**, R2526 (1997).
[24] M. J. Nandor and L. D. Van Woerkom, Phys. Rev. A **56**, 1273 (1997).
[25] S. X. Hu and Z. Z. Xu, Phys. Rev. A **56**, 3916 (1997); Appl. Phys. Lett. **71**, 2605 (1997).
[26] R. S. Mulliken, J. Chem. Phys. **7**, 20 (1939).
[27] T. Zuo, S. Chelkowski, and A. D. Bandrauk, Phys. Rev. A **49**, 3943 (1994).
[28] C. Cohen-Tannoudji, J. Dupont-Roc, and G. Grynstein, *Atom-Photon Interactions* (Wiley, New York, 1992), p. 207.
[29] F. Grossmann, P. Hänggi, Europhys. Lett. **18**, 571 (1992).
[30] J. M. Gomez and J. Plata, Phys. Rev. A **45**, 6954 (1992).
[31] Y. Kayanuma, Phys. Rev. B **47**, 9940 (1993).
[32] M. J. Moran, Phys. Rev. Lett. **69**, 2523 (1992).
[33] S. Hüller and J. Meyer-ter-Vehn, Phys. Rev. A **48**, 3906 (1993).
[34] J. D. Jackson, *Classical Electrodynamics* (Wiley, New York, 1962).
[35] A. D. Bandrauk and H. Shen, J. Chem. Phys. **99**, 1185 (1993).
[36] K. Burnett, V. C. Reed, J. Cooper, and P. L. Knight, Phys. Rev. A **45**, 3347 (1992).
[37] J. L. Krause, K. Schafer, and K. Kulander, Phys. Rev. A **45**, 4998 (1992).
[38] J. H. Eberly and M. V. Fedorov, Phys. Rev. A **45**, 4706 (1992).
[39] P. W. Atkins, *Molecular Quantum Mechanics* (Oxford University Press, London, 1985).
[40] M. Y. Ivanov, P. B. Corkum, and P. Dietrich, Laser Phys. **3**, 375 (1993).
[41] E. Aubanel, T. Zuo, and A. D. Bandrauk, Phys. Rev. A **49**, 3776 (1994).
[42] D. G. Lappas, M. V. Fedorov, and J. H. Eberly, Phys. Rev. A **47**, 1327 (1993).
[43] *Clusters of Atoms and Molecules*, edited by H. Haberland, Springer Series in Chemistry and Physics Vol. 52 (Springer, New York, 1994).
[44] H. Yu, T. Zuo, and A. D. Bandrauk, J. Phys. B **31**, 1533 (1998).
[45] W. M. Itano, J. J. Bellinger, J. N. Tan, B. Jelenkovicz, and D. J. Wineland, Science **279**, 686 (1998).
[46] J. N. Tan, J. J. Bellinger, B. Jelenkovicz, W. M. Itano, and D. J. Wineland, Phys. Rev. Lett. **72**, 4198 (1996).
[47] S. Chelkowski, C. Foisy, and A. D. Bandrauk, Phys. Rev. A **57**, 1176 (1998).